Journal of Applied Polymer Science

Improving the toughening in poly(lactic acid)-thermoplastic cassava starch reactive blends

Anibal Bher,[1,2,3] Rafael Auras ,[1] Carlos E. Schvezov[3]
[1]School of Packaging, Michigan State University, East Lansing, Michigan, USA, 48824
[2]Instituto Sabato, UNSAM-CNEA, San Martin, Buenos Aires, Argentina
[3]Instituto de Materiales de Misiones (IMAM), CONICET-UNaM, Posadas, Misiones, Argentina
Correspondence to: R. Auras (E-mail: aurasraf@msu.edu) and C. E. Schvezov (E-mail: schvezov@gmail.com)

ABSTRACT: Poly(lactic acid) (PLA), a physical blend of PLA and thermoplastic cassava starch (TPCS) (PLA-TPCS), and reactive blends of PLA with TPCS using maleic anhydride as compatibilizer with two different peroxide initiators [i.e., 2,5-*bis*(*tert*-butylperoxy)- 2,5-dimethylhexane (L101) and dicumyl peroxide (DCP)] PLA-*g*-TPCS-L101 and PLA-*g*-TPCS-DCP were produced and characterized. Blends were produced using either a mixer unit or twin-screw extruder. Films for testing were produced by compression molding and cast film extrusion. Morphological, mechanical, thermomechanical, thermal, and optical properties of the samples were assessed. Blends produced with the twin-screw extruder resulted in a better grade of mixing than blends produced with the mixer. Reactive compatibilization improved the interfacial adhesion of PLA and TPCS. Scanning electron microscopy images of the physical blend showed larger TPCS domains in the PLA matrix due to poor compatibilization. However, reactive blends revealed smaller TPCS domains and better interfacial adhesion of TPCS to the PLA matrix when DCP was used as initiator. Reactive blends exhibited high values for elongation at break without an improvement in tensile strength. PLA-*g*-TPCS-DCP provides promising properties as a tougher biodegradable film.
 J. Appl. Polym. Sci. **2017**, *135*, 46140.

KEYWORDS: biodegradable; biopolymers and renewable polymers; compatibilization; thermal properties; thermoplastics

Received 3 September 2017; accepted 3 December 2017
DOI: 10.1002/app.46140

INTRODUCTION

Poly(lactic acid) (PLA) is considered to be a promising substitute material for polymers from nonrenewable sources. PLA has applications in industries such as medical, packaging, automotive, and textile.[1] It is a biobased, recyclable, and compostable polymer with excellent optical and moderate barrier properties similar to polystyrene[2]; however, it shows brittle behavior with poor elongation at break and low modulus.[3] Blends of PLA with nonrenewable and renewable polymers have been extensively investigated, with the objective of improving its mechanical properties.[4–7] Physical and reactive blends of PLA with other biopolymers, such as thermoplastic starch (TPS) (starch plus a plasticizer), polycaprolactone, and polyhydroxyalkanoates, have been investigated to tailor mechanical, thermal, and barrier properties of PLA.[3,6,8,9]

Starch has extensively been used to produce TPS blends and films with several polymers, including PLA.[10] Starch has a chemical structure of branched (amylopectin) and linear (amylose) chains of glucose. A high presence of amylose produces stronger films.[11] Plasticization of starch is a very common technique to improve its mechanical and barrier properties.[10,12] Glycerol is common as a plasticizer.[12–14] Physical blends of starch and PLA show weak mechanical properties due to the poor compatibilization between the polymers, reflected by low interfacial adhesion. Blending PLA and starch with a high content of amylopectin resulted in blends with weak mechanical properties.[11] Reactive blends of PLA and TPS have been investigated to achieve a material with improved toughness and acceptable biodegradability. Among different types of starch, cassava starch is an excellent raw material. It is obtained from renewable sources and is used to produce different products such as glue, medicine matrix carriers, foods, and for packaging due to its low cost and abundance.[15] Cassava starch is inexpensive compared with corn starch, and is produced in large quantities in Nigeria, Thailand, and the northeast region of Argentina.[16] Cassava starch has a range of amylose between 20% and 30%, similar to values of corn, wheat, and potato. The low amylose content will produce weak films, so this drawback may be solved by reactive functionalization of thermoplastic cassava starch (TPCS) and PLA.

Additional Supporting Information may be found in the online version of this article.

Table I. Master Batches Produced with Mixer (MX)

	Composition (wt %)					Conditions		
Master batch	Neat PLA	Cassava starch	Glycerol	MA	L101 or DCP	*T* (°C)	RPM	*t* (min)
PLA-c	100	—	—	—	—	190	60	7
TPCS	—	70	30	—	—	120	100	7
PLA-*g*-MA	97.35	—	—	2	0.65	190	60	7
PLA-*g*-TPCS-L101-A	69.3	21	9	0.28	0.09	170	60	5
PLA-*g*-TPCS-DCP-A	69.63	21	9	0.28	0.09	170	60	5
PLA-*g*-TPCS-L101-B	69.63	21	9	0.28	0.09	170	60	5
PLA-*g*-TPCS-DCP-B	69.63	21	9	0.28	0.09	170	60	5

Blends of PLA and TPCS have been evaluated,[17–19] and the biodegradable blends showed enhanced mechanical properties. Since PLA is a hydrophobic material and starch is a hydrophilic material, physical blends of PLA and TPS are considered immiscible, with poor interfacial adhesion.[20,21] Alternative routes, such as reactive blending, are used to improve the compatibility of PLA and TPCS blends. Reactive blending is a common technique whereby a chemical grafting reaction between the polymers is generated during processing to improve compatibility.[22]

Reactive blending of PLA with TPCS using a compatibilizer, such as maleic anhydride (MA), and different peroxide initiators, such as 2,5-*bis*(*tert*-butylperoxy)-2,5-dimethylhexane (L101) and dicumyl peroxide (DCP), could improve interfacial adhesion and as a consequence the elongation at break. But reactive blending could also have side effects on the thermal properties and molecular structure.[17,20,23] Several researchers reported the use of compatibilizers and peroxide initiators for production of reactive blends of PLA and TPS.[17,19–21] MA is a common compatibilizer, extensively used for compatibilization of immiscible polymers.[24–26] One of the main advantages of using MA in PLA and TPCS reactive blends is that MA has high reactivity with PLA functional groups (i.e., carboxyl and hydroxyl groups at the end of the chains) in the presence of initiators such as L101 or DCP. The anhydride group of MA can react with the hydroxyl groups present in the starch.[27,28] MA also has low toxicity and is easy to handle.[23,29]

Several approaches have been used to evaluate the reactive compatibilization of PLA and TPS blends[30–33] but fewer with TPCS blends.[17,18,34] Therefore, a detailed study of the production of reactive blends of PLA and TPCS with different initiators using common processing techniques is needed. This work aimed to evaluate the performance of physical and reactive blends of PLA and TPCS regarding of mechanical, thermomechanical, optical, thermal, morphological, and molecular structure properties. Based on these characterizations, the primary goals of this research were to understand the different type of PLA/TPCS blend films obtained by each processing techniques; verify if reactive compatibilization is a suitable technique to improve the interfacial adhesion between the two immiscible phases as PLA and TPCS, and the role that it plays in final mechanical properties of the films. The blends were produced using a mixer (MX) and a twin-screw extruder (TSE), with MA as the compatibilizer, and L101 and DCP as peroxide initiators. The morphology of the physical and reactive blends was assessed to understand the domain distributions due to the reactive blending and processing conditions. Films were produced by compression molding (CM) and cast film extrusion (CF). Mechanical properties were evaluated for the samples considering cross and machine direction, and are reported and discussed.

EXPERIMENTAL

Materials

Cassava starch with amylose content of 25% ± 6% wt/wt and ~12% of moisture content was provided by Erawan Marketing Co., Ltd. (Bangkok, Thailand). Ingeo Biopolymer 2003D Poly(96% L-lactic acid) (PLA) was provided by NatureWorks LLC (Minnetonka, MN). Glycerol (>99.5%), MA, DCP, and L101 were all procured from Sigma-Aldrich (Milwaukee, WI). The PLA resin was dried under vacuum (67 kPa) at 50 °C overnight before using. All other materials were used as received.

Production of Master Batch

Production Using a MX Unit. Cassava starch and glycerol were premixed (70/30% wt) and held for 12 h before compounding. To produce TPCS, cassava starch was mixed with glycerol in a MX, a Brabender ATR Plasticorder (C.W. Brabender Instruments, Inc., South Hackensack, NJ). The final blends were fabricated following two procedures. In the first procedure (A), all the components [i.e., 30% TPCS, 56% PLA, 14% compatibilizer of PLA with MA (PLA-*g*-MA) 2% wt MA and 0.65% L101 or 0.65% DCP all by wt], were premixed in a plastic bag and introduced at the same time into the MX. In the second procedure (B), PLA-*g*-MA (2% wt MA) was first produced using two different initiators, L101 and DCP (0.65% wt). Then, a final blend with a composition of 56% PLA, 14% PLA-*g*-MA, and 30% TPCS, all by wt, was produced. Table I shows the blend compositions and the processing conditions.

TSE Production. PLA-*g*-MA was produced in a TSE, a Century ZSK-30 (Century, Traverse City, MI) using the same composition as in the MX (2% wt MA and 0.65% wt L101 or DCP, based on PLA weight). PLA, MA, and L101 or DCP were premixed in a bag before processing. The TSE residence time for a rate of feed of 70 g min^{-1} was ~3 min.

The configuration of the screws was (from feed to die): (1) feeding-melting zone; (2) large kneading/mixing zone; (3) conveying zone; (4) short kneading zone; and (5) conveying zone.[35]

Table II. Composition and Processing Parameters for Master Batches Produced with Twin-Screw Extruder (TSE)

Master batch	Composition (wt %)	Temperature profile from feed to the die (°C)	Screw speed (RPM)
PLA-c	100	140/150/160/160/160/170/170/170/170/160	120
TPCS	100	25/100/105/110/115/120/120/120/115/115	125
PLA-*g*-MA	98/2	140/150/160/160/160/170/170/170/170/160	120
PLA-TPCS	70/30	140/150/160/160/160/170/170/170/170/160	120
PLA-*g*-TPCS-L101	56/14/30[a]	140/150/160/160/160/170/170/170/170/160	120
PLA-*g*-TPCS-DCP	56/14/30[a]	140/150/160/160/160/170/170/170/170/160	120

[a] 14% wt is PLA-*g*-MA.

The extruded mass was pelletized in a BT 25 pelletizer (Scheer Bay Co., Bay City, MI), held in an oven at 50 °C for 3 h to remove residual water, and stored in a freezer at −15 °C until use. PLA-c (considered as control), TPCS, PLA-TPCS, and PLA-*g*-TPCS were also produced, pelletized, and stored as previously described (procedure B for MX). Table II shows the composition and processing conditions of the blends produced in the TSE.

Production of Films

Compression Molding. Master batches obtained from the two methods (MX and TSE) as indicated in Tables I and II, respectively, were compression molded in a hot press (PHI, City of Industry, CA). Three grams of each blend were placed between aluminum foil sheets and preheated for 10 min before compression. Compression molded films were produced with a temperature of 130 °C for TPCS and 150–160 °C for all the other samples; pressing time was 3 min at 33 MPa pressure. After production, the samples were stored at −15 °C until further use.

Cast Film (CF) Extrusion. Master batches obtained from TSE were used to produce cast films in a single extruder (Randcastle Extrusion Systems, Inc., Cedar Grove, NJ). Before the CF process, all the materials were conditioned overnight in an oven at 50 °C. Films were produced as indicated in Table III. The fabricated films were stored at −15 °C for further characterization.

Sample Characterization

Molecular Weight. Samples of PLA-c, PLA-TPCS, and PLA-*g*-TPCS using L101 or DCP (approximately 10 mg) as an initiator were dissolved in tetrahydrofuran (Pharmco-Aaper, Brookfield, CT) in a proportion of 2 mg mL^{-1}, and then held at room temperature until fully dissolved (∼24 h). The solution was then filtered through a 13 mm (diameter) 0.45 μm (pore size) poly(tetrafluoroethylene) filter (Acrodisc, Waters Corporation, Milford, MA). Finally, 100 μL of the filtrate was injected into a Waters gel permeation chromatograph (Waters Corp.), equipped with a Waters 1515 isocratic HPLC pump, a Waters 717 plus autosampler, four Waters Styragel columns (HR1, HR2, HR3, and HR4), and a Waters 2414 refractive index detector interface. Tetrahydrofuran was used as the mobile phase at a flow rate of 1 mL min^{-1}. A runtime of 50 min was used for each sample and an oven temperature of 35 °C for the detector and column. The number average molecular weight (M_n), weight average molecular weight (M_w), and polydispersity index (PI) were determined using the Waters Breeze 2 software version 6.20 (Waters Corp.). Polystyrene standards (Waters Shodex SM-105) were used for the calibration curve. Values of K and α of 0.000174 mL g^{-1} and 0.736, respectively, for PLA dissolved in tetrahydrofuran at 30 °C, were used to estimate the absolute M_n and M_w according to the Mark-Houwink equation.[36]

Morphology. Scanning electron microscopy (SEM) was used to investigate the morphology of the samples. Bar specimens of PLA-c, PLA-TPCS, and PLA-*g*-TPCS blends were produced with CM using pellets from TSE. Bars were immersed in liquid nitrogen for ∼3 min, then fractured by hand, treated with hydrochloric acid (6*N*) for 6 h to remove the TPCS phase,[37] and air dried for 12 h in a fume hood.[17] Finally, the samples were mounted on aluminum stubs using carbon suspension cement (SPI Supplies, West Chester, PA). Samples of films evaluated before and after tensile testing were mounted on aluminum stubs with high vacuum carbon tabs (SPI Supplies) and coated with iridium at a thickness of ∼2.7 nm. Samples were examined in a JEOL 6610LV (tungsten hairpin emitter) SEM (JEOL Ltd., Tokyo, Japan) at various magnifications at 10 kV. Area and diameter of the TPCS phase were determined using open source software ImageJ 1.50i.[38]

Table III. Film Samples Produced and Cast Film Extrusion (CF) Parameters Used

Films samples	Temperature profile from feed to the die (°C)	Screw speed (RPM)	Nip roller speed (RPM)	Winding roller speed (RPM)
PLA-c	140/150/160/160/160/170/168	30	50	12
PLA-TPCS	140/150/160/160/160/170/168	30	50	12
PLA-*g*-TPCS-L101[a]	140/150/160/160/160/170/168	30	50	12
PLA-*g*-TPCS-DCP[a]	140/150/160/160/160/170/168	30	50	12

[a] 14% wt is PLA-*g*-MA.

Table IV. M_n, M_w, and PI of PLA-c and PLA Portion of the Films Produced by Various Methods

Films samples	M_n (kDa)	M_n reduction (%)	M_w (kDa)	M_w reduction (%)	PI
		Mixer-compression molding			
PLA-c	89.6 ± 1.4^{a}	—	162.4 ± 1.1^{a}	—	1.8 ± 0.0^{a}
PLA-*g*-TPCS-L101-A	86.8 ± 1.2^{a}	3.1	$152.8 \pm 1.1^{a,b}$	5.9	1.8 ± 0.0^{a}
PLA-*g*-TPCS-DCP-A	$76.5 \pm 1.1^{a,b}$	14.6	146.9 ± 0.1^{b}	9.5	1.9 ± 0.0^{b}
PLA-*g*-TPCS-L101-B	60.3 ± 6.1^{c}	32.7	132.5 ± 5.2^{c}	18.4	2.2 ± 0.1^{c}
PLA-*g*-TPCS-DCP-B	$65.3 \pm 4.0^{b,c}$	27.1	134.7 ± 3.1^{c}	17.1	$2.2 \pm 0.2^{b,c}$
		Twin screw extrusion-compression molding			
PLA-c	92.4 ± 6.1^{a}	—	154.1 ± 2.2^{a}	—	1.7 ± 0.1^{a}
PLA-TPCS	52.9 ± 1.2^{b}	42.7	104.7 ± 3.4^{b}	32.1	2.0 ± 0.1^{b}
PLA-*g*-TPCS-L101	45.2 ± 1.3^{b}	51.1	84.6 ± 0.9^{c}	45.1	$1.9 \pm 0.0^{a,b}$
PLA-*g*-TPCS-DCP	48.3 ± 2.3^{b}	47.7	95.5 ± 1.9^{b}	38.0	2.0 ± 0.1^{b}
		Twin screw extrusion-cast film extrusion			
PLA-c	111.5 ± 1.3^{a}	—	181.4 ± 1.9^{a}	—	1.6 ± 0.0^{a}
PLA-TPCS	$107.3 \pm 10.9^{a,c}$	3.8	170.7 ± 7.6^{a}	5.9	1.6 ± 0.1^{a}
PLA-*g*-TPCS-L101	$78.6 \pm 17.4^{b,c}$	29.5	$130.7 \pm 7.2^{b,c}$	27.9	1.7 ± 0.3^{a}
PLA-*g*-TPCS-DCP	$89.8 \pm 6.6^{b,c}$	19.5	$140.1 \pm 5.4^{b,c}$	22.8	1.6 ± 0.0^{a}

Within a column and for the same processing method, values followed by a different letter are significantly different at $P \leq 0.05$ (Tukey's test).

Mechanical Properties. Tensile strength, elongation at break, and Young's modulus were evaluated using an Instron Universal Machine 5565 (Instron, Norwood, MA) according to ASTM D882-12.[39] Film samples were cut into 2.54 cm × 20 cm strips and conditioned for 48 h in a growth chamber (Environmental Growth Chambers, Chagrin Falls, OH) at 23 °C and 50% relative humidity. PLA-c and TPCS were tested with an initial grip, and rate grip separation of 125 mm and 12.5 mm min^{-1} and 50 mm and 500 mm min^{-1}, respectively. All the other samples were tested with an initial grip and rate grip separation of 100 mm and 50 mm min^{-1}, respectively. Five samples were evaluated for each formulation. Thickness of the films was determined by averaging five measurements for every specimen using a digital micrometer (Testing Machines Inc., Ronkonkoma, NY).

Thermomechanical Properties. Dynamic mechanical analysis was conducted using a RSA-G2 (TA Instruments, New Castle, DE). Samples (64 mm × 12 mm) were conditioned at 50% relative humidity and 23 °C for 48 h. Five specimens were evaluated for each type of blend. Storage modulus (E'), and tan δ were evaluated. A loading gap of 15 mm for a rectangular geometry was used. A tension axial force of 400 g with a sensitivity of 10 g was used with an oscillation temperature ramp of 3 °C min^{-1} from 25 to 100 °C with a frequency of 1.0 Hz and a strain of 2%.

Thermal Properties. Samples obtained from TSE and CM were evaluated in a differential scanning calorimeter (DSC) Q100 (TA Instruments) equipped with a mechanical cooling system and in a thermal gravimetric analyzer (TGA) Q50 (TA Instruments). For DSC, specimens between 5 and 10 mg were cut, weighed, and sealed in an aluminum pan. Samples were first cooled from room temperature to −50 °C, heated from −50 to 200 °C (first heating cycle), isothermal for 1 min at 200 °C, again cooled until −50 °C and finally heated to 200 °C (second heating cycle). The sample purge flow rate was 70 mL min^{-1} of nitrogen. Glass transition temperature (T_g), cold crystallization temperature (T_{cc}), melting temperature (T_m), and degree of crystallinity (X_c) of PLA and blends were analyzed using TA Universal Analysis 2000 software, version 4.5A. The X_c of PLA was calculated from an equation [eq. (1)] modified from Detyothin *et al.*[17]:

$$Xc = \frac{\Delta H_m - \Delta H_c}{\Delta H_f \times (1-\alpha)} \quad (1)$$

where ΔH_m and ΔH_c are the enthalpies of melting and crystallization, respectively; ΔH_f is the enthalpy of fusion of a pure crystalline PLA with a value of 93 J g^{-1},[40] α is the weight fraction of TPCS and MA in the final blends. The values of X_c are reported from the second heating run. Samples were run by triplicate.

For TGA, samples were evaluated under a nitrogen atmosphere with a flow rate of 60 mL min^{-1}. The method used was a ramp of 10 °C min^{-1} until reaching 600 °C using a platinum pan. Between 5 and 10 mg of sample was used for every run. Samples were run in triplicate.

UV–Visible Spectroscopy. Samples were evaluated by UV–visible spectroscopy using a Lambda 25 UV/Vis spectrophotometer (PerkinElmer, Waltham, MA). Transmittance was evaluated in a wavelength range of 190–880 cm^{-1} using one cycle, with a scan speed of 480 nm min^{-1}.

Statistical Analysis. Statistical analysis was conducted with MINITAB software (State College Park, PA). ANOVA and Tukey's test were used to evaluate the comparison of means at $P < 0.05$.

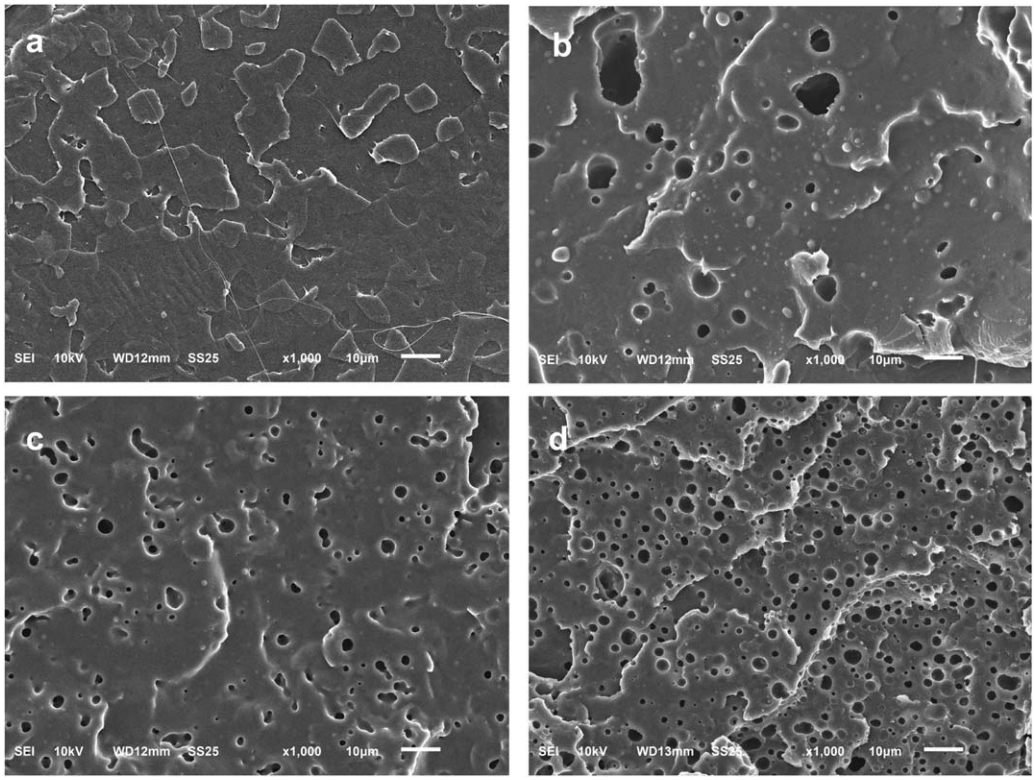

Figure 1. SEM images of PLA and reactive blends produced: (a) PLA-c, (b) PLA-TPCS, (c) PLA-*g*-TPCS-L101, (d) PLA-*g*-TPCS-DCP.

RESULTS AND DISCUSSION

PLA-c, TPCS, PLA-TPCS, and PLA-*g*-TPCS were produced using a MX and TSE. TSE was used to achieve a better grade of mixing for all the blends. Master batches from MX were used to produce films by CM, and those from TSE were used to produce films by CM and CF to understand the effect of processing methods on the morphological, mechanical, thermomechanical, thermal, and optical properties of the final blends.

Molecular Weight

Table IV presents the M_n, M_w, and PI of PLA-c, and the molecular weight of the PLA portion of the PLA-TPCS and PLA-*g*-TPCS films produced by the CM and CF methods.

Production of reactive blends (i.e., PLA-*g*-TPCS-L101 or PLA-*g*-TPCS-DCP) using MX-CM by procedures A and B resulted in significant differences in M_n, M_w, and PI when compared with PLA-c. Using procedure A, whereby PLA, TPCS, MA, and L101 or DCP were introduced all at once, avoided large reductions in M_n and M_w (less than 15%) due to less thermal processing. Producing PLA-*g*-MA (with L101 or DCP) first and then mixing with PLA and TPCS (procedure B) resulted in a larger reduction in M_n (~30%) and M_w (~18%) and an increase in PI due to the additional processing. With both procedures, the reductions in M_n and M_w could be attributed to the presence of free radicals created by the use of DCP and L101 as initiators. The reductions can also be attributed to chain scission of PLA resulting from the hydrolysis reactions of PLA-TPCS, since PLA-TPCS contains water and glycerol, which can degrade the PLA backbone. A greater increase in PI ($P \leq 0.05$) was found in samples produced by procedure B, due to the additional process. Detailed representation of the molecular weight distribution [$dW/d(\log(M_w)$ vs. log (M_w)] of the samples is provided in the Supporting Information available online. Supporting Information Figures S1 to S3 show the decrease and the widening of M_n. Additional discussion about the effect of processing using a MX on M_n, M_w, and PI of PLA blends can be found elsewhere.[20]

Reactive blends produced initially by TSE and followed by CM or CF had lower M_n and M_w than PLA-c ($P \leq 0.05$) (Table IV). PI for films produced by TSE-CF remained stable compared with PLA-c, likely due to the higher processing times (i.e., ~13 min for CM and ~10 min for CF). The presence of MA and the initiators (L101 or DCP) had an important effect on the reduction in M_n and M_w of PLA of these films, resulting in greater reductions in M_n and M_w for TSE-CM processed films, again likely due to the higher processing time that allowed for chain scissions and reaction with free radicals. PLA-*g*-TPCS films produced by CM, either by MX or TSE, had ~30% or ~50% reductions in M_n, respectively, when compared with PLA-c. The same trend was observed for M_w, with reduction percentages of ~20% and 40%, respectively. PLA-*g*-TPCS-DCP and PLA-*g*-TPCS-L101 films produced by TSE-CF showed 20% and 30% reductions in M_n, respectively, and 23% and 28% reductions in M_w, respectively.

Overall, lower reductions in M_n and M_w and no variation in PI were obtained for the films produced by TSE-CF, followed by MX-CM and TSE-CM. To confirm whether the compatibilization and modification of the interface were effective during these processes, the morphologies of the samples were evaluated.

Morphology

Figure 1 shows the morphology of the PLA matrix of the PLA-c and the blends produced by TSE, after removal of the starch

phase. The proportion of cavities can be correlated with the percentage of TPCS present in the PLA matrix. Figure 1(a) shows the morphology of PLA-c. In Figure 1(b), the physical blend of PLA-TPCS exhibits the presence of large cavities that represent a deficient compatibilization and distribution of TPCS domains into the PLA matrix. Incorporation of MA and the initiators L101 and DCP improved the interfacial adhesion between PLA and TPCS, as shown in Figure 1(c,d) where the distribution of TPCS was more homogenous [than in Figure 1(b)], with a substantial reduction in the size of TPCS domains. The use of DCP as an initiator achieved a better compatibilization of the interfaces, as seen in Figure 1(d) where the distribution of the TPCS domains was increased and the size of the TPCS phase was reduced compared with the physical and the reactive blends produced with L101 [Figure 1(c)]. Thus, reactive blending of PLA and TPCS with MA is a successful way to increase the interfacial adhesion and increase the compatibilization between two immiscible phases. In the presence of an initiator, MA can react with free radicals of PLA and TPCS reacts with carboxyl groups of PLA-*g*-MA. The reactive reaction increases the number of sites available where TPCS can linkage to PLA

Zhang and Sun[24] demonstrated a deficient compatibilization for physical and reactive blends of PLA and starch using MA and L101. Their physical blend exhibited the formation of edges and cavities between the starch and the PLA matrix, which was translated to low tensile strength. Huneault and Li,[23] also working with MA and L101, reported a significant decrease in the size of the TPS phase in reactive blends of PLA and TPS. They reported TPS domain size ranging from 5 to 30 μm for the physical blend and from 2 to 4 μm for the reactive blends, which showed more spherical holes and homogeneous distribution of the TPS phase. Their results were in agreement with those observed in Figure 1(b,c), which reveal TPCS domain sizes of 11.0 ± 2.6 and 7.0 ± 1.0 μm, respectively. Similar domains were found for L101; however, the amount of glycerol and TPCS used were different.[17] Wang *et al.*[33] reported similar findings for physical and reactive blends produced with MA and DCP; the average TPS domain size of the physical blend was ~10 μm and was easily removed from the fracture surface of the PLA matrix, leaving large cavities due to the lack of adhesion between the phases. On the other hand, the reactive blends showed a large improvement in dispersion and reduction of domain size of TPS in the PLA matrix; however, the TPS domain size was not quantified since the TPS phase was not extracted for SEM analysis. Similar findings were described by Wootthikanokkhan *et al.*[19]; however, they first grafted the MA on the TPS and then blended with PLA. In our study, the PLA-*g*-TPCS with DCP exhibited a TPS domain of 5.0 ± 1.3 μm, with a homogeneous distribution. A similar domain size was reported by Detyothin *et al.*[17] for reactive blends with the same concentration as in the present study but produced with L101. Other authors also observed a reduction of the TPS domain when producing reactive blends.[20,25,31,41] A reduction of domain size is indicative of better compatibilization between PLA and TPCS and could positively affect several properties of the reactive blends.

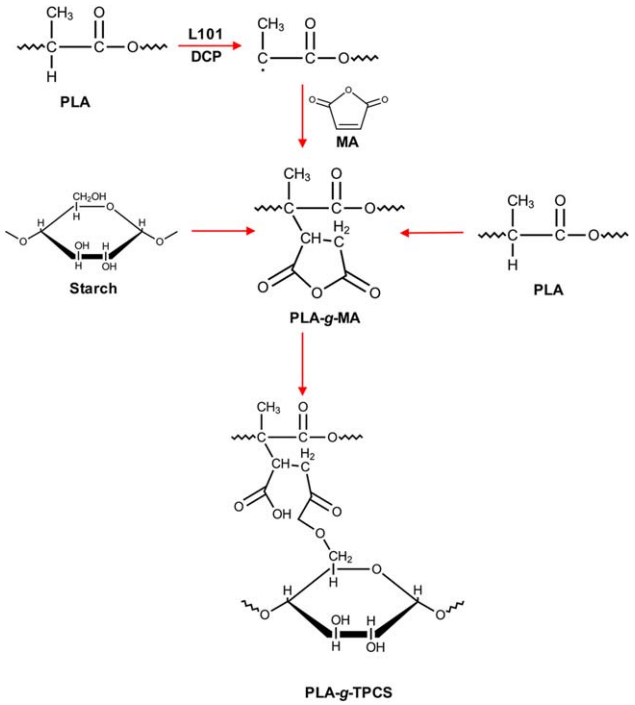

Scheme 1. Tentative reaction pathway of PLA-*g*-MA and PLA-*g*-TPCS with L101 or DCP, adapted from Zhang and Sun.[24] [Color figure can be viewed at wileyonlinelibrary.com]

Differences were observed between the cavity sizes and distribution of L101 [Figure 1(c)] and DCP [Figure 1(d)], indicating that DCP played a better role as initiator than L101. Scheme 1 shows the tentative reaction pathway with MA, using L101 or DCP, to produce PLA-*g*-MA and PLA-*g*-TPCS by addition of TPCS. Although the reaction routes are similar, TPCS domain sizes were smaller for PLA-*g*-TPCS blends [Figure 1(c,d)] than for PLA-TPCS [Figure 1(b)]. This result could be associated with the affinity between initiator and monomer, where the efficiency on grafting increases with more affinity. Figure S4 in the Supporting Information provides the TGA profile of L101 and DCP; DCP has higher thermal stability than L101. Pesetskii *et al.*,[42] working with free-radical grafting of itaconic acid onto low-density polyethylene, also reported significant differences for thermal stability of peroxides such as DCP and L101; DCP had a higher decomposition temperature(~131 °C) and complete decomposition temperature (~202 °C) than L101 (~118 and ~176 °C, respectively). Therefore, it is likely that the high volatility of L101 could diminish its role as initiator within the range of our processing temperatures, reducing the grafting of MA during processing.

Mechanical Properties

Figure 2 and Table V show the results for tensile properties of the films. Figure 2(a,b) show the results of the samples produced using the MX-CM and TSE-CM. Figure 2(c,d) shows the results of the samples produced using TSE-CF and evaluated in cross direction (CD) and machine direction (MD), respectively.

Similar elongation at break (~2%) were obtained for PLA-c films produced by MX-CM, TSE-CM, and TSE-CF (CD),

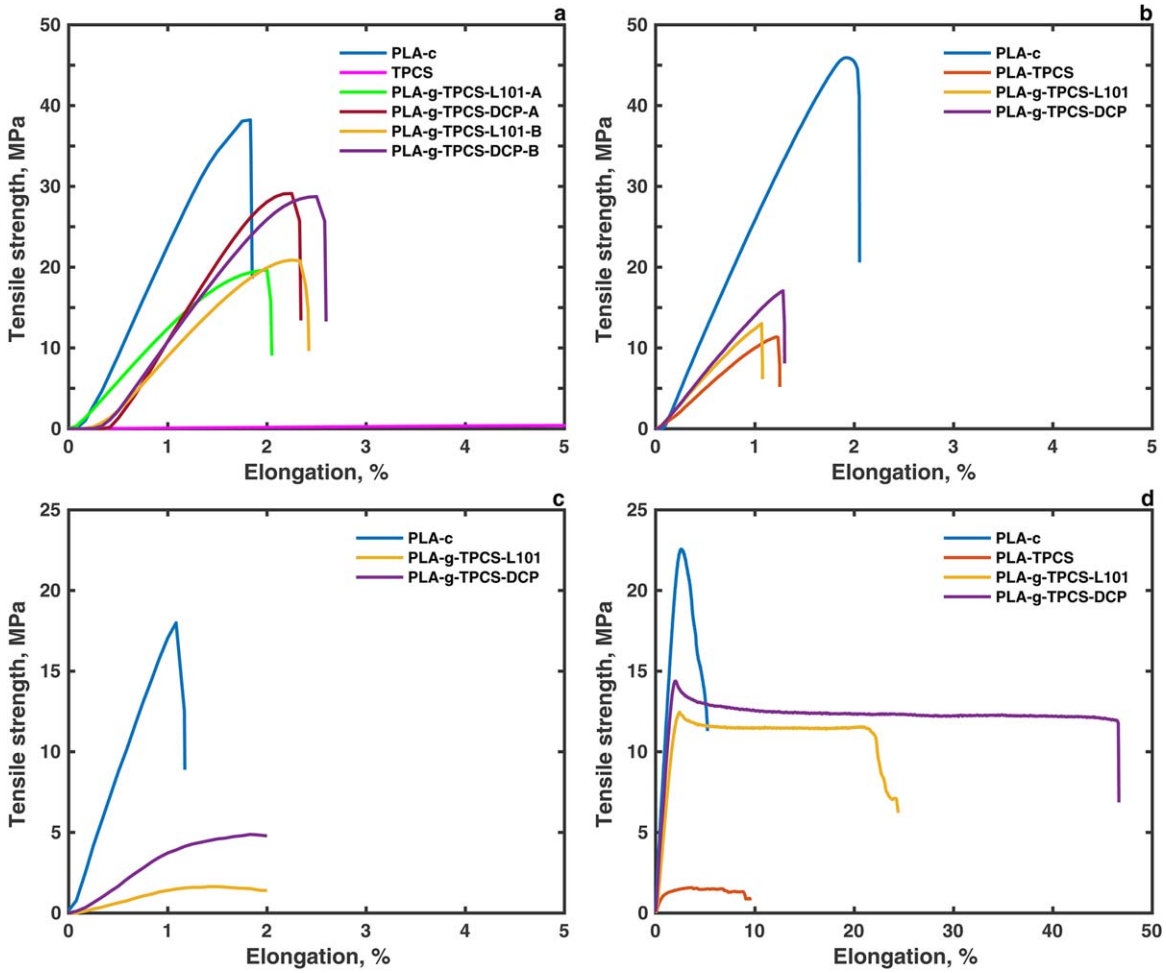

Figure 2. Tensile strength vs. elongation at break for films prepared by various methods: (a) mixer-compression molding, (b) twin-screw extrusion-compression molding, (c) twin-screw extrusion-cast film extrusion-cross direction, (d) twin-screw extrusion-cast film extrusion-machine direction. [Color figure can be viewed at wileyonlinelibrary.com]

whereas values were ~10% for TSE-CF (MD) (Table V). Tensile strength for PLA-c samples produced by MX-CM or TSE-CM were at least 100% higher than for those produced by TSE-CF, which is also reflected by the Young's modulus. This result may be attributed to variability in film thickness and the increase in crystallinity of these samples (see Table VI). Cicero *et al.*,[43] working with PLA fibers, showed that the modulus of PLA increased as the draw ratio increased. However, in this case, we observed that PLA-c samples produced by TSE-CF had much lower tensile strength than the MX-CM samples. Similar high tensile strength were reported by Hwang *et al.*[20] working with MX-CM samples.

TPCS produced by MX-CM [Figure 2(a)], had elongation at break of (~57%) but insignificant value of tensile strength (1.1 MPa). The incorporation of glycerol significantly affected the mechanical properties of the TPCS films due to its plasticizing effect. Alves *et al.*[12] explained that with the incorporation of glycerol, structural modifications occurred in the starch matrix, and as a consequence the film became less dense.

Tensile strength of PLA-*g*-TPCS samples produced by MX-CM was reduced compared with PLA-c, resulting in a modulus reduction. The high elongation at break provided by TPCS was not reflected in the PLA-*g*-TPCS blends when TPCS was incorporated into the PLA matrix by grafting. Samples of PLA-c and PLA-*g*-TPCS produced by MX-CM did not show a typical necking region, indicating that they were brittle and weak samples without a plastic deformation region. A similar behavior of low elongation at break and decreasing tensile strength for reactive blends was reported by Hwang *et al.*[20] Furthermore, PLA-*g*-TPCS produced by TSE-CM exhibited a similar trend of low tensile strength and elongation at break, as reported by Hwang *et al.*[20] [Figure 2(b)]. Therefore, processing can play a crucial role in the final properties of the reactive blend samples.

TPCS has very low tensile strength but very high elongation at break.[12] However, as depicted in Figure 2(b,d), there is an important reduction of the tensile strength and elongation at break for PLA-TPCS (physical blend) produced by TSE-CM and TSE-CF, respectively. This result is mainly due to the poor interfacial adhesion between the PLA and TPCS phases creating cluster or aggregation of each phases, as shown in Figure 1(b). Similar results were reported for physical blend, with the tensile strength two

Table V. Tensile Properties of Sample Produced by Various Methods

Samples	Thickness (μm)	Tensile strength (MPa)	Modulus (MPa)	Elongation at break (%)
Mixer-compression molding				
PLA-c	152.0 ± 2.7^{a}	51.2 ± 5.2^{a}	2680 ± 44^{a}	2.4 ± 0.3^{a}
TPCS	194.0 ± 5.4^{b}	1.1 ± 0.0^{b}	9.9 ± 0.6^{b}	56.9 ± 6.4^{b}
PLA-*g*-TPCS-L101-A	128.0 ± 3.3^{c}	19.3 ± 0.7^{c}	1360 ± 54^{c}	2.2 ± 0.4^{a}
PLA-*g*-TPCS-DCP-A	155.0 ± 5.0^{a}	27.4 ± 1.2^{d}	$1660 \pm 167^{c,d}$	2.3 ± 0.2^{a}
PLA-*g*-TPCS-L101-B	176.4 ± 13.9^{d}	$24.5 \pm 6.1^{c,d}$	$1620 \pm 408^{c,d}$	2.6 ± 0.7^{a}
PLA-*g*-TPCS-DCP-B	174.4 ± 9.3^{d}	28.4 ± 1.3^{d}	1760 ± 54^{d}	2.6 ± 0.3^{a}
Twin-screw extrusion-compression molding				
PLA-c	150.0 ± 18.7^{a}	44.6 ± 2.9^{a}	1930 ± 323^{a}	2.0 ± 0.1^{a}
PLA-TPCS	156.7 ± 10.3^{a}	11.5 ± 2.4^{b}	741 ± 142^{b}	1.2 ± 0.2^{b}
PLA-*g*-TPCS-L101	119.6 ± 9.5^{b}	12.3 ± 5.5^{b}	980 ± 130^{b}	1.1 ± 0.5^{b}
PLA-*g*-TPCS-DCP	124.4 ± 11.7^{b}	16.1 ± 3.5^{b}	700 ± 367^{b}	1.4 ± 0.2^{b}
Twin-screw extrusion-cast film extrusion-cross direction				
PLA-c	23.7 ± 1.7^{a}	19.6 ± 2.1^{a}	1764 ± 95^{a}	1.5 ± 0.3^{a}
PLA-*g*-TPCS-L101	49.1 ± 6.9^{b}	2.0 ± 0.7^{c}	200.0 ± 89.4^{c}	1.9 ± 0.1^{a}
PLA-*g*-TPCS-DCP	50.0 ± 4.1^{b}	5.9 ± 0.9^{b}	530 ± 149^{b}	$2.1 \pm 0.1b^{a}$
Twin-screw extrusion-cast film extrusion-machine direction				
PLA-c	24.2 ± 3.5^{a}	22.5 ± 2.6^{a}	1180 ± 83^{a}	6.0 ± 1.1^{a}
PLA-TPCS	151.2 ± 6.3^{c}	1.57 ± 0.3^{c}	172.0 ± 37.9^{c}	11.6 ± 1.2^{b}
PLA-*g*-TPCS-L101	46.0 ± 5.6^{b}	11.9 ± 2.0^{b}	780 ± 130^{b}	23.4 ± 2.1^{c}
PLA-*g*-TPCS-DCP	51.6 ± 5.5^{b}	10.5 ± 5.8^{b}	920 ± 130^{b}	48.7 ± 2.1^{d}

Within a column and for the same processing method, values followed by a different letter are significantly different at $P \leq 0.05$ (Tukey's test).

Table VI. T_g, T_{cc}, T_m, and X_c as Obtained by the First and Second Heating Cycle of the DSC

	First heating cycle				Second heating cycle			
Samples	T_g (°C)	T_{cc} (°C)	T_m (°C)	X_c (%)	T_g (°C)	T_{cc} (°C)	T_m (°C)	X_c (%)
Mixer-compression molding								
PLA-c	58.9 ± 0.4^{a}	124.1 ± 0.3^{a}	149.0 ± 0.3^{a}	1.1 ± 0.1^{a}	61.5 ± 0.1^{a}	127.5 ± 0.2^{a}	149.6 ± 0.2^{a}	1.0 ± 01^{a}
PLA-*g*-TPCS-L101-A	54.2 ± 0.3^{b}	$109.2 \pm 1.6^{b,c}$	145.3 ± 0.8^{a}	0.6 ± 0.6^{a}	59.1 ± 0.2^{b}	127.7 ± 0.5^{a}	147.4 ± 0.1^{b}	3.5 ± 1.0^{a}
PLA-*g*-TPCS-DCP-A	53.4 ± 0.3^{b}	113.5 ± 1.0^{b}	145.2 ± 0.6^{a}	9.8 ± 4.4^{b}	59.4 ± 0.0^{b}	—	148.2 ± 0.1^{c}	3.7 ± 0.7^{a}
PLA-*g*-TPCS-L101-B	54.3 ± 0.6^{b}	$104.1 \pm 1.1^{c,d}$	142.7 ± 0.2^{a}	22.7 ± 2.3^{c}	58.2 ± 0.0^{c}	114.5 ± 0.3^{b}	144.9 ± 0.1^{d}	2.1 ± 1.0^{a}
PLA-*g*-TPCS-DCP-B	53.7 ± 2.2^{b}	101.8 ± 2.9^{d}	145.8 ± 3.3^{a}	26.2 ± 2.6^{c}	58.4 ± 0.1^{c}	122.5 ± 1.6^{c}	146.4 ± 0.3^{e}	3.7 ± 1.7^{a}
Twin-screw extrusion-cast film extrusion								
PLA-c	60.9 ± 0.8^{a}	91.9 ± 3.7^{a}	151.0 ± 0.6^{a}	7.8 ± 6.0^{a}	60.7 ± 0.3^{a}	125.7 ± 0.5^{a}	149.9 ± 0.6^{a}	3.1 ± 0.4^{a}
PLA-TPCS	$57.9 \pm 1.5^{a,b}$	102.3 ± 0.6^{b}	146.1 ± 3.0^{b}	10.8 ± 3.6^{a}	57.3 ± 0.4^{b}	112.4 ± 0.7^{b}	144.0 ± 0.3^{b}	0.2 ± 0.2^{b}
PLA-*g*-TPCS-L101	54.0 ± 2.9^{b}	107.0 ± 0.9^{b}	143.4 ± 0.2^{b}	13.2 ± 6.9^{a}	56.9 ± 0.5^{b}	120.1 ± 1.3^{c}	146.8 ± 0.4^{c}	1.2 ± 1.0^{b}
PLA-*g*-TPCS-DCP	55.3 ± 0.2^{b}	104.2 ± 1.6^{b}	143.4 ± 0.3^{b}	25.6 ± 7.2^{a}	56.9 ± 0.2^{b}	122.6 ± 1.1^{c}	146.6 ± 0.4^{c}	2.8 ± 0.3^{a}

Within a column and for the same processing method, values followed by a different letter are significantly different at $P \leq 0.05$ (Tukey's test).

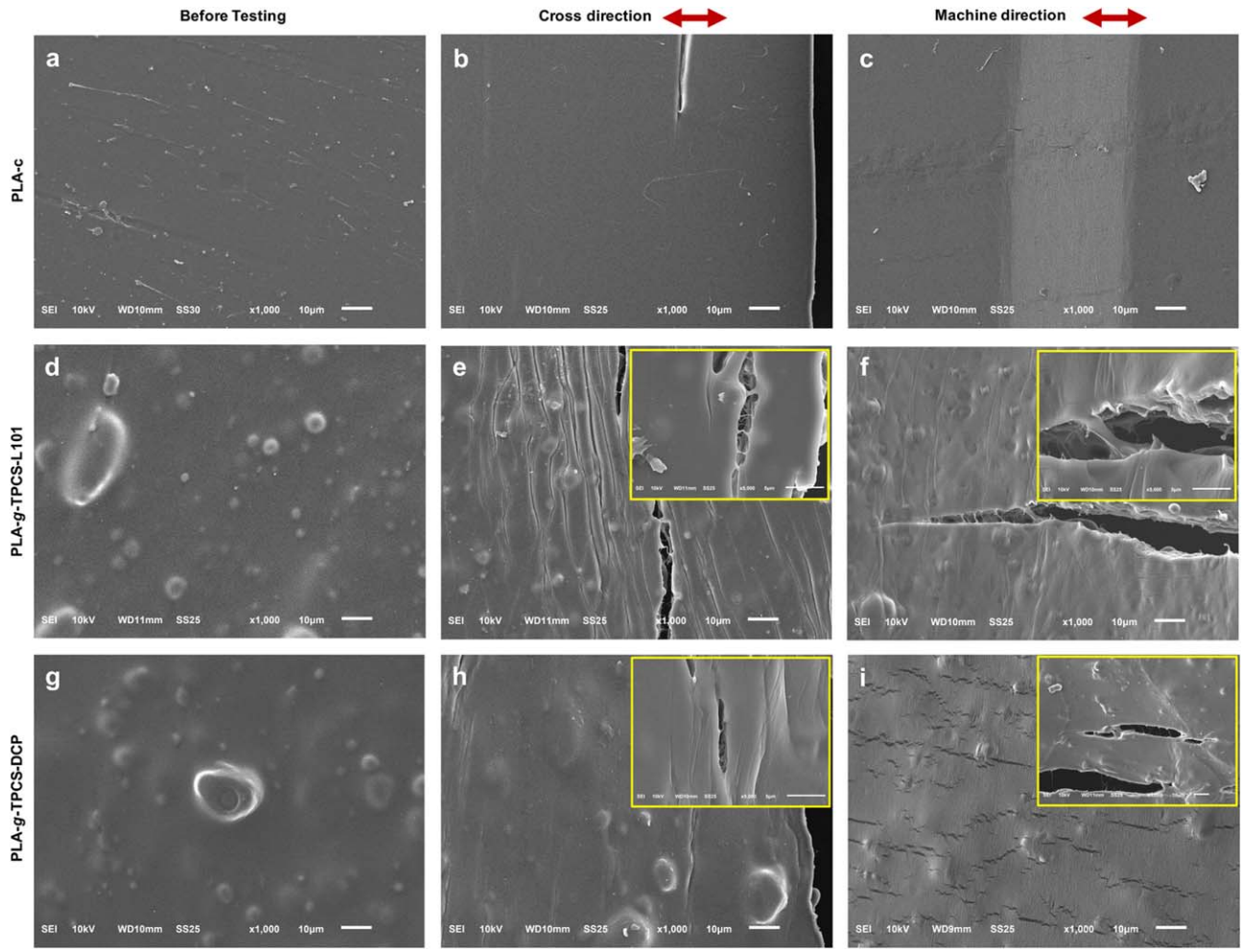

Figure 3. SEM images of PLA and reactive blend samples: (a) PLA-c, (b) PLA-c-CD, (c) PLA-c-MD, (d) PLA-*g*-TPCS-L101, (e) PLA-*g*-TPCS-L101-CD, (f) PLA-*g*-TPCS-L101-MD, (g) PLA-*g*-TPCS-DCP, (h) PLA-*g*-TPCS-DCP-CD, (i) PLA-*g*-TPCS-DCP-MD. Insets of e,f,h,i represent magnification of the respective images. Arrow indicates direction of the tensile test. [Color figure can be viewed at wileyonlinelibrary.com]

times lower than for PLA.[17] Nezamzadeh *et al.*,[25] working with TPS, also found a reduction in tensile strength and elongation at break for PLA-TPS blends, but did not find the same results for Young's moduli, which remained similar to neat PLA. PLA-TPCS films were difficult to produce by CF due to the nucleation of micro holes and cracks, which were then responsible for the lower tensile strength as shown in Figure 2(d).

Introduction of the compatibilizer (PLA-*g*-MA with L101 or DCP) and production of the reactive blends resulted in PLA-*g*-TPCS films that could be easily compressed or casted, resulting in better dispersion of the TPCS phase into the PLA matrix [Figure 1(c,d)]. The presence of MA resulted in a TPCS phase with smaller domains, which is evidence of low interfacial tension, as previously reported.[10,17,20] The use of DCP resulted in samples with higher tensile strength and elongation at break compared to the produced with L101 [Figure 2(a,c,d)]. As shown in Figure 1(d), the use of DCP decreased the size of the dispersion of the TPCS phase in the PLA matrix.

Samples produced by TSE-CF and evaluated in CD exhibited lower tensile strength [Figure 2(c)] and similar values of elongation at break than samples produced by either MX-CM or TSE-CM. Figure 2(d) shows the results for samples produced by TSE-CF and evaluated in MD. PLA-*g*-TPCS blends showed high values for elongation at break. However, PLA-*g*-TPCS produced with DCP showed a higher value of elongation at break than the other blends. As discussed previously, Scheme 1 shows that the pathways for the grafting reactions for L101 and DCP are similar. Therefore, differences observed in elongation at break and also morphology characterization (Figure 1) could be associated with the solubility and affinity between the peroxide and the monomer (PLA).[42] Samples of the PLA-*g*-TPCS blends produced by the TSE-CF method and evaluated in MD [Figure 2(d)] exhibited a higher elongation at break than the specimens evaluated in CD [Figure 2(c)], demonstrating that blends produced by TSE-CF are tougher. It can be concluded that the samples produced by MX-CM and TSE-CM do not achieve the same type of morphology in the final PLA-*g*-TPCS blends as those produced by TSE-CF. Therefore, the final properties of reactive blends produced by MX-CM and TSE-CM do not reflect the real values (high elongation at break) to be obtained by TSE and CF for these blends during industrial production.

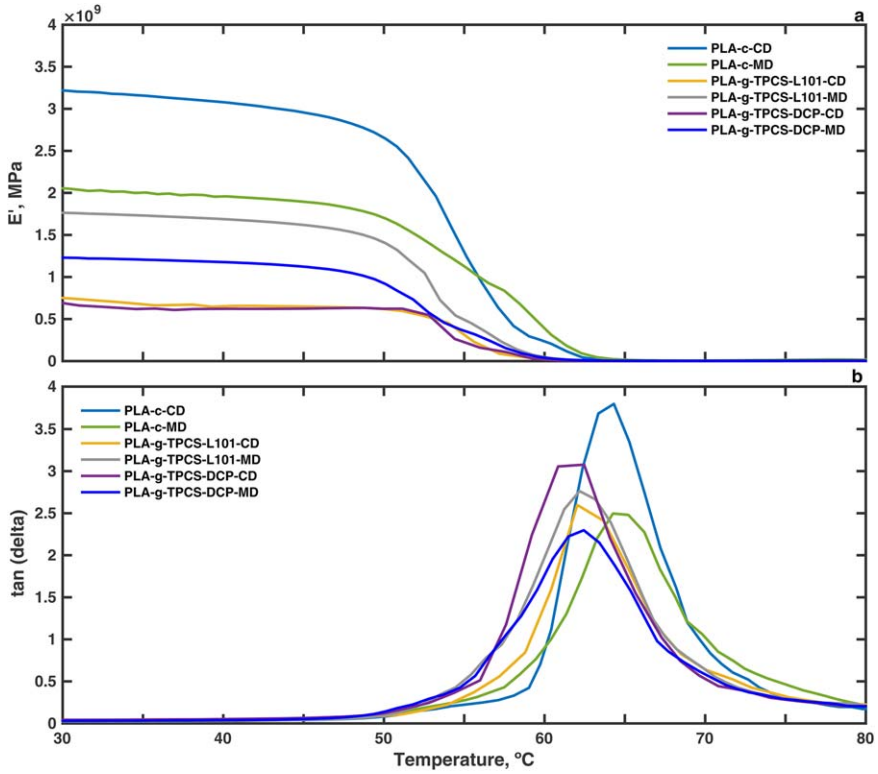

Figure 4. DMA thermograms of the PLA samples produced by twin-screw extrusion-cast film extrusion: (a) E', storage modulus, and (b) tan δ. [Color figure can be viewed at wileyonlinelibrary.com]

This difference can be attributed to the better mixing obtained by TSE and the orientation achieved during CF.

Figure 3 shows SEM images of the films produced by TSE before and after tensile testing applied in the CD and MD. Before testing, the presence of the TPCS phase in the PLA-*g*-TPCS films [as previously described in Figure 1(c,d)] is apparent [Figure 3(d,g)] compared with the control [Figure 3(a)]. After testing in CD the control film developed lines of fracture perpendicular to the tension direction with a clean cut [Figure 3(b)], and PLA-*g*-TPCS-L101-CD [Figure 3(e)] and PLA-*g*-TPCS-DCP-CD [Figure 3(h)] displayed detachment of the TPCS and PLA phases. This detachment could result in a small gain of elongation at break [as noted in Figure 2(c)]. However, the tensile strength was reduced due to the presence of the TPCS. The presence of rugosity or perpendicular lines to the tension direction indicates a progressive mode of failure. The insets of Figure 3(e,h) reveal the detachment of the phases perpendicular to the force direction, with formation of small breaches. After testing in MD, PLA-c-MD [Figure 3(c)] shows lines of fracture parallel to the tension direction and band whitening of the samples due to stress. For PLA-*g*-TPCS-L101-MD [Figure 3(f)] and PLA-*g*-TPCS-DCP-MD [Figure 3(i)], the detachment of the TPCS and PLA phases occurred parallel to the tension direction, which in this case contributes to a large gain of elongation at break with a small reduction of tensile strength. The insets of Figure 3(f,i) reveal the detachment of the phases in the tension direction, with formation of small breaches. When the PLA-*g*-TPCS films are oriented in the MD, TPCS rubbery phase and cavities that formed in the PLA matrix acted as a toughening phase during tension. The formation of small cavities during fracture in the PLA-*g*-TPCS-DCP-MD [Figure 3(i)] seems to provide a better toughening behavior than the large cavity formation for the PLA-*g*-TPCS-L101-MD [Figure 3(f)]. This result may be due to better adhesion and compatibilization of the DCP than the L101 [as shown in Figure 1(c,d)], creating a stronger interphase between TPCS and the PLA matrix, which resulted in greater toughness. Similar results were reported by Chapleau *et al.*[41] for polylactide/thermoplastic blends.

Thermomechanical Properties

The storage modulus (E'), and tan δ of the samples produced by TSE-CF and evaluated in CD and MD were compared. Reactive blends evaluated in CD and MD demonstrated a lower stiffness (lower E') than PLA-c evaluated either in CD or MD [Figure 4(a)]. The addition of TPCS improved the flexibility of the reactive blends in the range of temperature assessed, and the incorporation of MA as a compatibilizer enhance the interaction in the matrix of PLA/TPCS blends.[33] Hwang *et al.*,[20] working with different compositions of TPS, found the same trend of decreasing E' for reactive blends of PLA and starch. A significant decrease in E' was observed for PLA-c and PLA-*g*-TPCS blends at about 55 °C. Similar behavior for PLA and reactive blends was found by Detyothin *et al.*[17] using MA and L101. The plot of tan δ [Figure 4(b)] indicates higher values of T_g (not shown) in comparison with the values obtained by DSC (Table VI). This result may be due to different measurement techniques, as previously reported.[44,45] Reactive blends resulted in a shifting of tan δ peaks to lower temperatures respect to

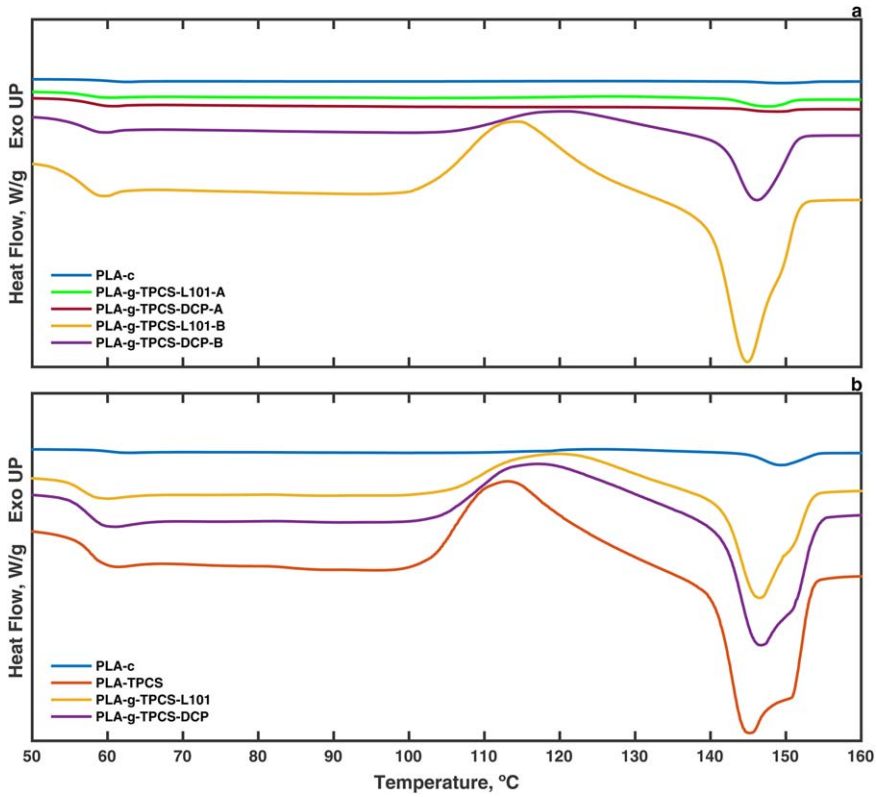

Figure 5. DSC thermograms of the second heating cycle of the tested PLA film samples: (a) samples produced by mixer and compression molding, (b) samples produced by twin-screw extrusion and compression molding. [Color figure can be viewed at wileyonlinelibrary.com]

PLA. The shift of these peaks could be attributed to the presence of TPCS increasing the molecular chain mobility of reactive blends respect to PLA, reflected in lower values of T_g.

The E' for PLA-*g*-TPCS with L101 and DCP in the MD were higher than in the CD in the measured temperature range, indicating a toughening behavior in the MD. This finding is in agreement with results obtained from tensile testing [Figure 2(c,d)]. However, a similar trend was not observed for PLA-c. Therefore, the presence of TPCS plays a dual role during MD orientation: increasing elongation at break and increasing the modulus of the reactive blends.

Thermal Properties

Table VI summarizes the thermal property values obtained by the first and second heating cycles of the DSC for all films. Figure 5 illustrates the thermal properties from the second heating cycle of the DSC. For films produced by MX-CM, PLA-c had a T_g ~61 °C [Figure 5(a)]; the reactive blends produced either with L101 or DCP had a similar T_g but 1 °C lower than neat PLA for procedure A, and 2 °C lower than neat PLA for procedure B. The small reduction observed for T_g values could be related with two factors. First, the lower M_n observed for the reactive blends produced with either procedure A and B (Table IV) could increase the mobility of the PLA chains, as described by the Flory–Fox equation.[46] Second, the presence of TPCS and low M_n oligomers of the compatibilizer (PLA-*g*-MA) could have a plasticizing effect, as previously reported.[47] A similar trend in the reduction of T_g for reactive blends of PLA and TPS was reported elsewhere.[17,20,25] For procedure A, T_{cc} was evident only for the blend produced with L101, with a similar value to PLA-c. Blends produced with L101 and DCP using procedure B had T_{cc} values of ~114 °C for L101 and 123 °C for DCP. The significantly reduction in T_{cc} for the blends produced by procedure B could be associated with an increase in mobility of PLA chains due to the reduction of M_n, and an early nucleation effect, as previously reported elsewhere.[31,47,48] Blends of PLA-*g*-TPCS-L101-B and PLA-*g*-TPCS-DCP-B had much larger cold crystallization values than the PLA-c and samples produced by procedure A. These results could be attributed to the increased in the chain mobility of the polymer due to the reduction of M_n and increase in nucleation (Table IV), which could be attributed to the presence of the PLA-*g*-MA either with L101 or DCP, as observed by Hwang *et al.*[20] All the MX-CM blends produced were mostly amorphous. PLA-c exhibited low X_c, which is in agreement with results from Martin and Avérous.[49] The X_c for PLA-*g*-TPCS blends produced from either procedure A or B were not significantly different. A small reduction in T_m was observed for PLA-*g*-TPCS-L101 and PLA-*g*-TPCS-DCP (procedures A and B) in comparison with PLA-c. Hwang *et al.*[20] working with reactive blends of PLA and TPS with MA and DCP, and Detyothin *et al.*[17] working with reactive blends of PLA and TPCS with MA and L101, found double melting peaks for DSC thermograms, which were attributed to the formation of α and α′ crystals. In our study, the double melting peaks were not as evident without further deconvolution of the melting peaks.

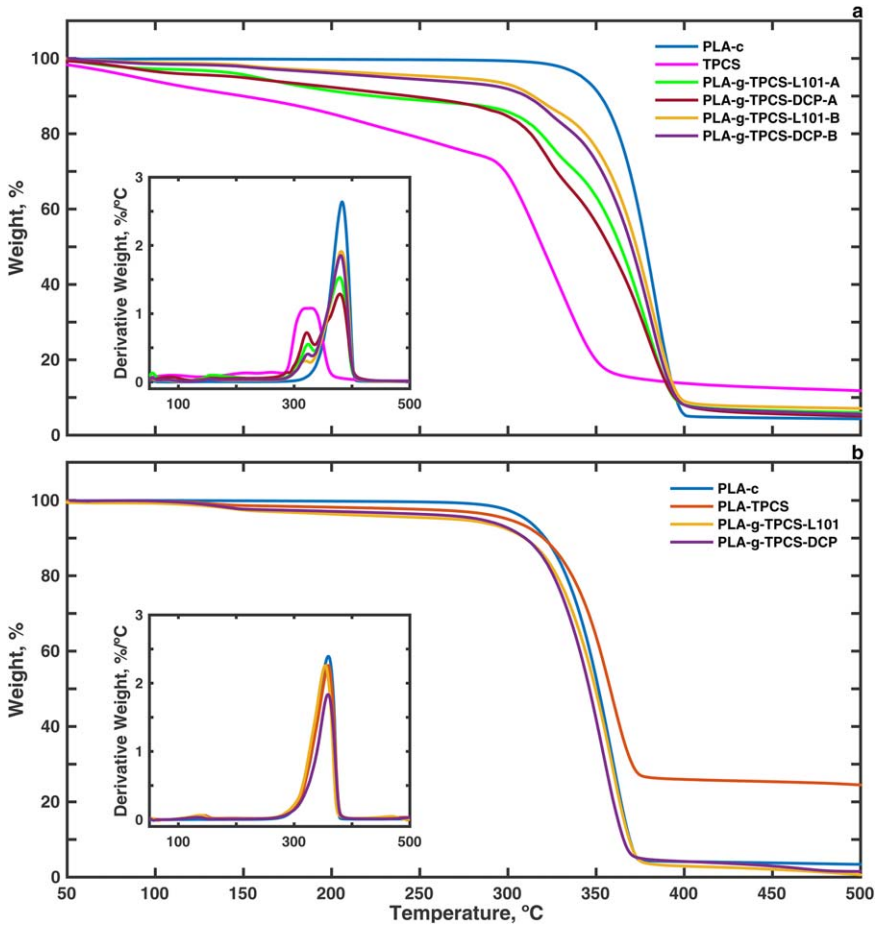

Figure 6. TGA thermograms of the tested samples: (a) samples produced by mixer-compression molding, (b) samples produced by twin-screw extrusion-cast film extrusion; inset shows the differential thermogravimetry (DTG) curves obtained for the different samples. [Color figure can be viewed at wileyonlinelibrary.com]

All films produced by TSE-CF exhibited lower T_g than the comparable blends produced by MX-CM [Figure 5(b), Table VI]. These findings could be attributed to deficient mixing reached with the MX and a higher degradation during TSE processing, allowing a large reduction of M_n, which resulted in a reduction of T_g. A decrease of ~3 °C was observed in the T_g of PLA-TPCS and PLA-*g*-TPCS blends produced by TSE-CF compared with PLA-c, which could be associated with the plasticizing effect of the glycerol contained in the TPCS.[50] Although we expected a slightly larger reduction of T_g for the PLA-*g*-TPCS L101 or DCP with respect to PLA-TPCS due to the use of the compatibilizer PLA-g-MA with L101 or DCP, there was no significant difference ($P > 0.05$) in the T_g of these blends. Hwang *et al.*[20] reported a decrease in T_g of the reactive blends with respect to the physical blends when investigating the compatibilizing effect of MA on PLA and TPS reactive blends. A large decrease in T_{cc} was observed for the physical and reactive blends in comparison with PLA-c [Figure 5(b)]. All the samples produced were mostly amorphous, with values of X_c of ~0. The same results were obtained by XRD (as shown in Figure S5 in the Supporting Information). Compared with PLA-c the T_m of PLA-*g*-TPCS and PLA-TPCS decreased by ~3 to 5 °C, respectively.

Figure 6 shows the TGA results for thermal stability analysis of PLA-c, TPCS, PLA-TPCS, and PLA-*g*-TPCS blends. PLA-*g*-TPCS blends produced by procedures A and B [Figure 6(a)] exhibited an onset decomposition temperature of ~300 °C, which is lower than the onset temperature of PLA-c (~350 °C). TPCS exhibited an initial weight loss due the evaporation of water, and a decomposition temperature of ~300 °C. The final weight loss for the blends was ~94% for PLA-c, 91% for TPCS, 96% for PLA-*g*-TPCS blends with DCP and L101 using procedure A, 93% for PLA-*g*-TPCS blend with DCP using procedure B, and 97% for PLA-*g*-TPCS with L101 using procedure B. The onset decomposition temperatures of the blends decreased with the addition of TPCS due to the poor thermal stability of starch in comparison with neat PLA.[20] A larger reduction in the onset decomposition temperature was observed for the reactive blends produced by MX-CM using procedure A than for samples produced by procedure B. Addition of the compatibilizer in procedure B improved the thermal stability of the reactive blends. Also, the better mixing in TSE achieved a better compatibility and thermal stability for the final blends. Hwang *et al.*[20] indicated that the maleation reaction had little effect on the thermal stability of the reactive blends. Orozco *et al.*[21] also reported that the stability of blends was not significantly affected due to the

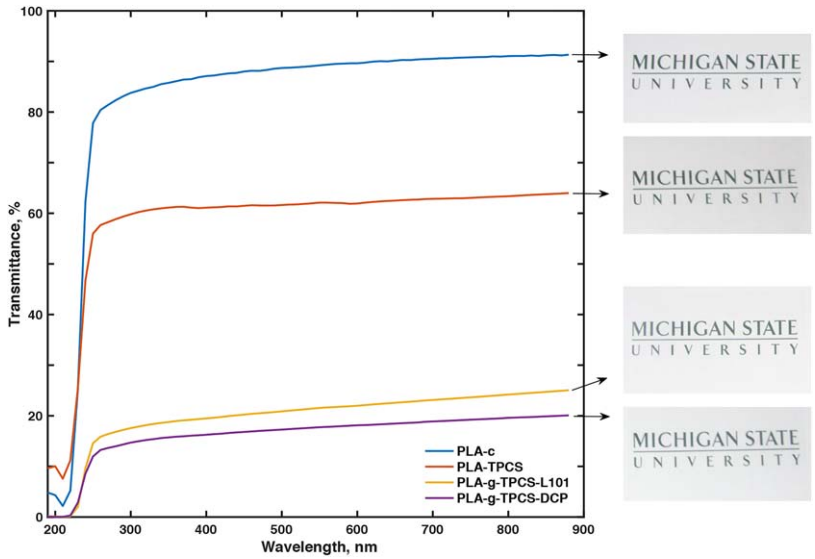

Figure 7. %Transmittance and optical images of PLA film samples produced by twin-screw extrusion-cast film extrusion. [Color figure can be viewed at wileyonlinelibrary.com]

compatibilization and modification of the PLA matrix. However, Figure 6(b) indicates that the addition of the compatibilizer (L101 and DCP) in the PLA-*g*-TPCS (procedure B) resulted in improved thermal stability of the reactive blends, likely due to better compatibilization of the final structure and a smoother degradation as also suggested by FTIR plots in Figures S6–S8 of the Supporting Information.

Insets of Figure 6 show the differential thermogravimetry (DTG) curves for the different samples. In the inset of Figure 6(a), a broad peak for TPCS with a bimodal peak (around 310 and 340 °C) could be associated with the decomposition of amylose and amylopectin, respectively. For the PLA-*g*-TPCS blends produced either using procedure A or B, a first overlapped peak at ~310 °C is due to the decomposition of starch; a second peak at ~380 °C is assigned to the pyrolysis of PLA. The inset of Figure 6(b) shows a complete overlap among curves of PLA, PLA-TPCS, and PLA-*g*-TPCS blends. Detyothin *et al.*[17] found similar results when working with reactive blends of PLA-*g*-TPCS and L101. This full overlap of the DTG curves could be attributed to the better mixing obtained with the TSE, and confirms the better physical and reactive blends obtained.

UV–Visible Properties

Blockage of the UV-B and C light wavelength range (<315 nm) is highly desirable to avoid oxidation reactions of the film products. Development of transparent but UV-blockage biobased films is currently highly sought after for consumer applications. Figure 7 presents the light transmittance (%*T*) for the CF films produced. The %*T* of PLA-c, PLA-TPCS, PLA-*g*-TPCS-L101, and PLA-*g*-TPCS-DCP was ~80%, 50%, 16%, and 14%, respectively, at 300 nm, and 90%, 55%, 20%, and 18%, respectively, at 600 nm (Table S1, Supporting Information). Transmittance was reduced in all the films produced with TPCS, compared to PLA-c. Mali *et al.*[14] explained that the opacity of starch films is mostly related to the amylose content, and could be related to the distribution of starch. In this study, the TPCS used to produce the physical and reactive blends had ~25% ± 6% of amylose. At the lower range in the UV-C region (180–220 nm), %*T* values were 10% for PLA-c and PLA-TPCS, whereas PLA-*g*-TPCS blends blocked all transmittance at this range. However, in the range of 220–240 nm, there was a significant increase in %*T* to ~80% for PLA-c and ~60% for PLA-TPCS. Similar values of transmittance were reported for PLA-c.[8] A ~25% decrease in transparency was found between 230 and 880 nm for PLA-TPCS samples compared with PLA-c. PLA-*g*-TPCS blends produced with DCP or L101 had transmittance values of ~20% in the region of 250–880 nm. The large reduction in %*T* compared with PLA-c indicated a good distribution of TPCS in the PLA matrix. The reduction in %*T* of PLA-TPCS and PLA-*g*-TPCS compared with PLA-c was mainly due to the presence of starch granules in the matrix of PLA, which would diffract the visible light due to the size domains of the TPCS phase. Reactive blend films had much lower %*T* values than the physical blend films (Figure 7) due to better distribution and compatibilization of the TPCS granules in the PLA matrix [as shown in Figure 1(c,d)]. This reduction in %*T* was reflected in the haze values of the samples, with a reduction of ~50% for PLA-TPCS and ~70% for PLA-*g*-TPCS blends (Table S1, Supporting Information). Müller *et al.*[51] found low values of transmittance (~1%) for PLA films compounded with 30% TPCS (v/v) using a single extruder and CM, which they largely attributed to the heterogeneous structure of the samples due to lower miscibility between the polymer phases. PLA-TPCS and PLA-*g*-TPCS films exhibited an increase in the yellowness index of ~13% (Table S1, Supporting Information), as also observed visually. The opacity values reported for the films were in accordance with transmittance values (Table S1, Supporting Information), with a large increase for the reactive blend films. The low value reported for PLA-TPCS was associated with two factors: the presence of holes in the film, which reduced the absorbance, and the presence of starch granules that increased the thickness of the film. Although the PLA-*g*-TPCS films produced with

L101 or DCP exhibited lower transmission of visible light and slightly higher yellowness, which could be concealed with printing, they can be highly acceptable for medical and consumer applications since they are still transparent and provide additional protection to UV light, as shown in Figure 7.

CONCLUSIONS

The production and characterization of physical and reactive blends of PLA and TPCS were reported. PLA and reactive blends of PLA with TPCS were prepared by two different techniques, MX and TSE films were produced either by CM or CF. The films produced by MX-CM and TSE-CM did not have the same mechanical properties as films produced by TSE-CF. Production of films using TSE and CF are common commercial techniques. The production of films using MX-CM is useful for research purpose; however, the obtained reactive blend films do not reflect industrial scale techniques and their properties are not the same either. Use of MA as a compatibilizer improved the interfacial adhesion between PLA and TPCS with a larger improvement of blends produced with the initiator DCP rather than L101. Mechanical properties showed an increase in the elongation at break for samples of the reactive blends evaluated in the MD. Orientation plays an important role in these samples since the tensile properties evaluated with samples produced with MX-CM, TSE-CM, and considering CD for CF (TSE-CF-CD) did not show any improvement of elongation at break. The presence of a plastic phase in the PLA-*g*-TPCS allowed larger deformation of the samples produced by TSE and CF and tested in the MD. PLA-*g*-TPCS-DCP is a good formulation as a reactive blend. However, further research is needed for producing commercial films where tougher and compostable films are required. Future work should be conducted in a one-step continuous process, by using a TSE with a sheet film die at the end of the barrel. This technological improvement could avoid the molecular degradation of PLA and TPCS due to the use of a second CF processing step. Furthermore, activities will be focused on understanding the changes in barrier properties and compostability due to the addition of TPCS in PLA.

Processing by MX or twin-screw extrusion follow by CM resulted in films with poor molecular structure and mechanical properties, demonstrating that these techniques do not achieve the expected mixing result. However, TSE processing follow by CF obtained samples that were properly mixed and compatibilized. Reactive compatibilization improved the interfacial adhesion of PLA and TPCS as shown by the formation of small domains in reactive blends in comparison with the physical blend. Reactive compatibilized processed by TSE-CF extrusion showed an improvement in elongation at break.

ACKNOWLEDGMENTS

The authors thank the Center for Advanced Microscopy at Michigan State University (MSU) for assisting with the SEM images, the Michigan Biotechnology Institute (at MSU) for providing access to the twin-screw extruder, and the Center for Crystallographic Research (at MSU) for allowing the use of the XRD Diffractometer. A.B. thanks the Consejo Nacional de Investigaciones Cientificas y Tecnicas (CONICET) in Argentina for providing financial support through a Ph.D. fellowship, and the School of Packaging at MSU for partial financial support.

REFERENCES

1. Murariu, M.; Dubois, P. *Adv. Drug Delivery Rev.* **2016**, *107*, 17.
2. Castro-Aguirre, E.; Auras, R.; Selke, S.; Rubino, M.; Marsh, T. *Polym. Degrad. Stab.* **2017**, *137*, 251.
3. Lim, L. T.; Auras, R.; Rubino, M. *Prog. Polym. Sci.* **2008**, *33*, 820.
4. Castro-Aguirre, E.; Iñiguez-Franco, F.; Samsudin, H.; Fang, X.; Auras, R. *Adv. Drug Delivery Rev.* **2016**, *107*, 333.
5. Maharana, T.; Pattanaik, S.; Routaray, A.; Nath, N.; Sutar, A. K. *React. Funct. Polym.* **2015**, *93*, 47.
6. Detyothin, S.; Kathuria, A.; Jaruwattanayon, W.; Selke, S. E. M.; Auras, R. Poly(lactic acid): Synthesis, Structures, Properties, Processing, and Applications; Wiley: Hoboken, NJ, **2010**; p 227.
7. Saini, P.; Arora, M.; Kumar, M. N. V. R. *Adv. Drug Delivery Rev.* **2016**, *107*, 47.
8. Auras, R.; Harte, B.; Selke, S. *Macromol. Biosci.* **2004**, *4*, 835.
9. Farah, S.; Anderson, D. G.; Langer, R. *Adv. Drug Delivery Rev.* **2016**, *107*, 367.
10. Nafchi, A. M.; Moradpour, M.; Saeidi, M.; Alias, A. K. *Starch/Stärke* **2013**, *65*, 61.
11. Tharanathan, R. N. *Trends Food Sci. Technol.* **2003**, *14*, 71.
12. Alves, V. D.; Mali, S.; Beléia, A.; Grossmann, M. V. E. *J. Food Eng.* **2007**, *78*, 941.
13. Mali, S.; Sakanaka, L. S.; Yamashita, F.; Grossmann, M. V. E. *Carbohydr. Polym.* **2005**, *60*, 283.
14. Mali, S.; Karam, L. B.; Ramos, L. P.; Grossmann, M. V. E. *J. Agric. Food Chem.* **2004**, *52*, 7720.
15. Auras, R.; Arroyo, B.; Selke, S. *Starch/Stärke* **2009**, *61*, 463.
16. Shetty, J. K.; Strohm, B. A.; Lee, S. H.; Duan, G.; Bates, D. *Ind. Biotechnol.* **2014**, *10*, 275.
17. Detyothin, S.; Selke, S. E. M.; Narayan, R.; Rubino, M.; Auras, R. A. *J. Appl. Polym. Sci.* **2015**, *132*, DOI: 10.1002/app.42230.
18. Soares, F. C.; Yamashita, F.; Müller, C. M. O.; Pires, A. T. N. *Polym. Test.* **2013**, *32*, 94.
19. Wootthikanokkhan, J.; Kasemwananimit, P.; Sombatsompop, N.; Kositchaiyong, A.; Isarankura na Ayutthaya, S.; Kaabbuathong, N. *J. Appl. Polym. Sci.* **2012**, *126*, E389.
20. Hwang, S. W.; Shim, J. K.; Selke, S.; Soto-Valdez, H.; Rubino, M.; Auras, R. *Macromol. Mater. Eng.* **2013**, *298*, 624.
21. Orozco, V. H.; Brostow, W.; Chonkaew, W.; López, B. L. *Macromol. Symp.* **2009**, *277*, 69.
22. Detyothin, S.; Selke, S. E. M.; Narayan, R.; Rubino, M.; Auras, R. *Polym. Degrad. Stab.* **2013**, *98*, 2697.
23. Huneault, M. A.; Li, H. *Polymer* **2007**, *48*, 270.
24. Zhang, J. F.; Sun, X. *Biomacromolecules* **2004**, *5*, 1446.

25. Ali Nezamzadeh, S.; Ahmadi, Z.; Afshari Taromi, F. *J. Appl. Polym. Sci.* **2017**, *134*, DOI: 10.1002/app.44734.
26. Yang, Y.; Tang, Z.; Xiong, Z.; Zhu, J. *Int. J. Biol. Macromol.* **2015**, *77*, 273.
27. Carlson, D.; Nie, L.; Narayan, R.; Dubois, P. *J. Appl. Polym. Sci.* **1999**, *72*, 477.
28. Mani, R.; Bhattacharya, M.; Tang, J. *J. Polym. Sci. Part A: Polym. Chem.* **1999**, *37*, 1693.
29. Raquez, J. M.; Narayan, R.; Dubois, P. *Macromol. Mater. Eng.* **2008**, *293*, 447.
30. Chen, L.; Qiu, X.; Xie, Z.; Hong, Z.; Sun, J.; Chen, X.; Jing, X. *Carbohydr. Polym.* **2006**, *65*, 75.
31. Yu, L.; Petinakis, E.; Dean, K.; Liu, H.; Yuan, Q. *J. Appl. Polym. Sci.* **2011**, *119*, 2189.
32. Akrami, M.; Ghasemi, I.; Azizi, H.; Karrabi, M.; Seyedabadi, M. *Carbohydr. Polym.* **2016**, *144*, 254.
33. Wang, N.; Yu, J.; Ma, X. *Polym. Int.* **2007**, *56*, 1440.
34. Teixeira, E. D. M.; Curvelo, A. A. S.; Corrêa, A. C.; Marconcini, J. M.; Glenn, G. M.; Mattoso, L. H. C. *Ind. Crops Prod.* **2012**, *37*, 61.
35. Nabar, Y.; Narayan, R.; Schindler, M. *Polym. Eng. Sci.* **2006**, *46*, 438.
36. Dorgan, J. R.; Janzen, J.; Knauss, D. M.; Hait, S. B.; Limoges, B. R.; Hutchinson, M. H. *J. Polym. Sci. Part B: Polym. Phys.* **2005**, *43*, 3100.
37. Li, H.; Huneault, M. A. *J. Appl. Polym. Sci.* **2011**, *122*, 134.
38. Schneider, C. A.; Rasband, W. S.; Eliceiri, K. W. *Nat. Methods* **2012**, *9*, 671.
39. ASTM International. D882-12. Standard Test Method for Tensile Properties of Thin Plastic Sheeting; ASTM: West Conshohocken, PA, **2012**; p 11.
40. Fischer, E. W.; Sterzel, H. J.; Wegner, G. *Polymere* **1973**, *251*, 980.
41. Chapleau, N.; Li, H.; Huneault, M. A. *Int. Polym. Process* **2011**, *22*, 402.
42. Pesetskii, S. S.; Jurkowski, B.; Krivoguz, Y. M.; Kelar, K. *Polymer* **2001**, *42*, 469.
43. Cicero, J. A.; Dorgan, J. R.; Garrett, J.; Runt, J.; Lin, J. S. *J. Appl. Polym. Sci.* **2002**, *86*, 2839.
44. Gracia-Fernández, C. A.; Gómez-Barreiro, S.; López-Beceiro, J.; Tarrío Saavedra, J.; Naya, S.; Artiaga, R. *Polym. Test.* **2010**, *29*, 1002.
45. Brostow, W.; Chiu, R.; Kalogeras, I. M.; Vassilikou-Dova, A. *Mater. Lett.* **2008**, *62*, 3152.
46. Fox, T. G.; Flory, P. J. *J. Polym. Sci.* **1954**, *14*, 315.
47. Jang, W. Y.; Shin, B. Y.; Lee, T. J.; Narayan, R. *J. Ind. Eng. Chem.* **2007**, *13*, 457.
48. Li, H.; Huneault, M. A. *Polymer* **2007**, *48*, 6855.
49. Martin, O.; Averous, L. *Polymer* **2001**, *42*, 6209.
50. Park, J. W.; Im, S. S.; Kim, S. H.; Kim, Y. H. *Polym. Eng. Sci.* **2000**, *40*, 2539.
51. Müller, P.; Bere, J.; Fekete, E.; Moczo, J.; Nagy, B.; Kallay, M.; Gyarmati, B.; Pukanszky, B. *Polymer* **2016**, *103*, 9.